



OPEN ACCESS

EDITED BY

Eduard Murani,
Leibniz-Institute for Farm Animal Biology (FBN),
Germany

REVIEWED BY

Klaus Jung,
University of Veterinary Medicine Hannover,
Germany

Tara G. McDanel,
Agricultural Research Service (USDA),
United States

*CORRESPONDENCE

Matthew A. Scott
✉ matthewscott@tamu.edu

RECEIVED 04 August 2023

ACCEPTED 20 September 2023

PUBLISHED 05 October 2023

CITATION

Bigelow RA, Richeson JT, McClurg M,
Valeris-Chacin R, Morley PS, Funk JL and
Scott MA (2023) Characterizing the influence of
various antimicrobials used for metaphylaxis
against bovine respiratory disease on host
transcriptome responses.

Front. Vet. Sci. 10:1272940.

doi: 10.3389/fvets.2023.1272940

COPYRIGHT

© 2023 Bigelow, Richeson, McClurg, Valeris-Chacin, Morley, Funk and Scott. This is an open-access article distributed under the terms of the [Creative Commons Attribution License \(CC BY\)](https://creativecommons.org/licenses/by/4.0/). The use, distribution or reproduction in other forums is permitted, provided the original author(s) and the copyright owner(s) are credited and that the original publication in this journal is cited, in accordance with accepted academic practice. No use, distribution or reproduction is permitted which does not comply with these terms.

Characterizing the influence of various antimicrobials used for metaphylaxis against bovine respiratory disease on host transcriptome responses

Rebecca A. Bigelow¹, John T. Richeson¹, Molly McClurg², Robert Valeris-Chacin², Paul S. Morley², Jenna L. Funk² and Matthew A. Scott^{2*}

¹Department of Agricultural Sciences, West Texas A&M University, Canyon, TX, United States,

²Veterinary, Education, Research, and Outreach Program, School of Veterinary Medicine and Biomedical Sciences, Texas A&M University, Canyon, TX, United States

Currently, control against bovine respiratory disease (BRD) primarily consists of mass administration of an antimicrobial upon arrival to facility, termed “metaphylaxis.” The objective of this study was to determine the influence of six different antimicrobials used as metaphylaxis on the whole blood host transcriptome in healthy steers upon and following arrival to the feedlot. One hundred and five steers were stratified by arrival body weight (BW=247±28kg) and randomly and equally allocated to one of seven treatments: negative control (NC), ceftiofur (CEFT), enrofloxacin (ENRO), florfenicol (FLOR), oxytetracycline (OXYT), tildipirosin (TILD), or tulathromycin (TULA). On day 0, whole blood samples and BW were collected prior to a one-time administration of the assigned antimicrobial. Blood samples were collected again on days 3, 7, 14, 21, and 56. A subset of cattle ($n=6$) per treatment group were selected randomly for RNA sequencing across all time points. Isolated RNA was sequenced (NovaSeq 6,000; ~35M paired-end reads/sample), where sequenced reads were processed with ARS-UCD1.3 reference-guided assembly (HISAT2/StringTie2). Differential expression analysis comparing treatment groups to NC was performed with glmmSeq (FDR ≤ 0.05) and edgeR (FDR ≤ 0.1). Functional enrichment was performed with KOBAS-i (FDR ≤ 0.05). When compared only to NC, unique differentially expressed genes (DEGs) found within both edgeR and glmmSeq were identified for CEFT ($n=526$), ENRO ($n=340$), FLOR ($n=56$), OXYT ($n=111$), TILD ($n=3,001$), and TULA ($n=87$). At day 3, CEFT, TILD, and OXYT shared multiple functional enrichment pathways related to T-cell receptor signaling and Fc ϵ RI-mediated NF- κ B activation. On day 7, Class I major histocompatibility complex (MHC)-mediated antigen presentation pathways were enriched in ENRO and CEFT groups, and CEFT and FLOR had DEGs that affected IL-17 signaling pathways. There were no shared pathways or Gene Ontology (GO) terms among treatments at day 14, but TULA had 19 pathways and eight GO terms enriched related to NF- κ B activation, and interleukin/interferon signaling. Pathways related to cytokine signaling were enriched by TILD on day 21. Our research demonstrates immunomodulation and potential secondary therapeutic mechanisms induced by antimicrobials commonly used for metaphylaxis, providing insight into the beneficial anti-inflammatory properties antimicrobials possess.

KEYWORDS

bovine respiratory disease, metaphylaxis, antimicrobial, transcriptome, RNA-Seq, immune, cattle, T-cell

1. Introduction

Bovine respiratory disease (BRD) is a multifactorial disease complex that has been identified as the cause of approximately 75% of morbidity and over 50% of mortality in the feedlot industry (1, 2). The pathogenesis of BRD culminates from the interactions between stressors and environmental risk factors, viral and bacterial pathogens, and the host immunological response (3). Due to the structure of the beef cattle marketing system, calves are exposed to multiple stressors at once, which can result in host immunosuppression. A viral infection allows for pathogenic bacteria to induce a secondary infection, contributing to the development of BRD (4). Moreover, current BRD diagnosis in the field is subjective, based on visual assessment of clinical signs associated with BRD, and has previously been shown to have poor sensitivity (5, 6). As such, metaphylaxis, or the mass administration of injectable antimicrobials upon facility arrival, is an effective method of controlling BRD (7). With the rise of antimicrobial resistance (AMR), exploring mechanisms of how drugs influence host immunological responses is imperative to understanding how they remain efficacious (8). Examining the host whole blood transcriptome and differential gene expression provides insight to novel genomic mechanisms associated with immune response to antimicrobial administration.

RNA sequencing (RNA-Seq) produces quantitative and qualitative data regarding RNA in a biologic sample. It accomplishes this by combining high-throughput sequencing methodology with computational analysis to quantify transcripts in an RNA extraction (9). This technology can be used to identify transcribed genes within a cell or tissue, genomic activity at a particular time, and associated mechanisms being up- or downregulated over time. RNA-Seq has been used to examine development of BRD in multiple tissues against different pathogens, differences between sick versus healthy cattle, identification of potential biomarkers for BRD, and antimicrobial resistance genes among various bacteria (10–15). However, RNA-Seq has not been used to specifically investigate the impact of antimicrobial administration on the host immunological response through the whole blood transcriptome.

Therefore, the objective of this study was to evaluate the effect of six different antimicrobials used for metaphylaxis on the host whole blood transcriptome of healthy steers upon and following arrival to the feedlot. The findings of this study may provide a foundation for future research into secondary mechanisms identified as potential therapeutic opportunities for BRD.

2. Materials and methods

Animal procedures were approved by the West Texas A&M University (WTAMU) Institutional Animal Care and Use Committee before study initiation (IACUC protocol #2022.03.002). This research

was conducted from May 2022 to July 2022 at the WTAMU Research Feedlot, near Canyon, TX. This study was carried out in accordance with Animal Research: Reporting of *In Vivo* Experiments (ARRIVE) guidelines (16).

2.1. Arrival processing

A total of 105 crossbred steers (243 ± 23.9 kg) were acquired from a local grow yard facility in the panhandle of Texas. Previous health history records indicated that all cattle received tildipirosin (Zuprevo, Merck Animal Health, Madison, NJ), a trenbolone acetate and estradiol implant (Revalor-G implant, Merck Animal Health, Madison, NJ), an antiparasitic drug (Dectomax, Zoetis, Parsippany-Troy Hills, NJ), an IBR/BRSV/PI₃ vaccine (Nasalgen, Merck Animal Health, Madison, NJ), Synanthic oral dewormer (Boehringer Ingelheim, Ridgefield, CT), a Titanium 5 vaccine for IBR, BVD Types I and II, PI₃, and BRSV (Elanco Animal Health, Greenfield, IN), and a Bovilis Vision vaccine (Merck Animal Health, Madison, NJ) at label dosing during the start of their backgrounding period, 45 days prior to arrival at the WTAMU Research Feedlot. Prior to animal arrival and every sample collection day, the squeeze chute scale used in this study was validated by placing 45.54 kg (50-lb certified steel weights) on each side of the chute at a time until a total of 454 kg was validated. Upon arrival (day -1), individual body weight (BW) was recorded. Additionally, cattle were given identification ear tags and were confirmed to be negative for persistent infection with bovine viral diarrhea virus (BVDV) *via* ear notch antigen capture ELISA (PI; Cattle Stats, Oklahoma City, OK). Steers were placed in a single 124.8 m² pen together overnight with *ad libitum* access to water, a starter diet of 0.5% of their arrival BW, and coastal Bermuda grass hay at 0.5% arrival BW.

On day 0, individual BW were collected again and averaged with day -1 BW to determine initial BW. Whole blood samples were collected *via* jugular venipuncture into PAXgene Blood RNA tubes (QIAGEN, Germantown, MD) prior to a one-time administration of the assigned treatment at day 0. Nasopharyngeal swabs and fecal samples were also collected on day 0. Blood, BW, and nasopharyngeal swabs were collected again on days 3, 7, 14, 21, and 56, with fecal samples collected on days 21 and 56; nasopharyngeal swabs and fecal samples were collected for a separate study. Cattle were evaluated daily for bovine respiratory disease (BRD), or other signs of clinical disease, by a trained observer and assigned a clinical illness score for BRD (CIS: 0 to 4 scale). A CIS of 0 is described as a “normal” animal showing no clinical signs of illness. A CIS of 1 indicated “mild BRD” with elevated respiratory rate, mild-to-moderate anorexia, mild depressed attitude, and a shallow, dry cough when viewed at a distance. A CIS of 2 indicated a “moderate BRD” steer with a gaunt appearance, possible nasal and/or ocular discharge, mild-to-moderate muscle weakness and depressed attitude, and a persistent

shallow, dry cough. A steer assigned a CIS of 3 was considered “severe BRD” with labored breathing, purulent nasal and/or ocular discharge, productive coughing, loss of alertness, and severe depression. A CIS of 4 was deemed “moribund” that was unresponsive upon human approach, recumbent and unwilling to rise when approached, showed evidence of moderate-to-severe dehydration, and marked anorexia. Any steer deemed a CIS of a 1 or 2 was pulled and treated if the rectal temp recorded was $\geq 40^{\circ}$ C. A steer with a CIS of 3 or 4 was treated regardless of rectal temp recorded. If a steer was assigned a CIS of 4 and deemed unlikely to clinically recover by an on-site veterinarian, it was euthanized *via* AMVA-approved methods. If a steer was pulled but not treated, it was returned to its treatment pen. However, if a steer was pulled and treated, a blood sample, nasopharyngeal swab, and fecal sample were taken before removing the animal from trial. No cattle were pulled nor treated for clinical disease after their initial administration of treatment at any time throughout this 56-day trial.

2.2. Treatments and experimental design

The BWs collected on day -1 were used to randomly allocate cattle to experimental treatments with equal weights *via* Excel RANDBETWEEN function (Microsoft, Redmond, WA). Within each treatment pen, there were 15 individuals total. In the pens receiving antibiotics, ten individuals were randomly selected for the administration of antimicrobial treatment and five received no antimicrobial treatment, serving as sentinel controls within each treatment pen. Cattle within pens were randomly selected using a random number generator in Excel, selecting the five lowest values as sentinel controls *via* RANDBETWEEN function. This experiment consisted of seven treatment groups evaluated over a 56-day receiving period: (1) negative control, no antimicrobial administration (NC), (2) ceftiofur administered subcutaneously at the base of the ear at a dosage of 6.6 mg CE/kg BW (EXCEDE Sterile Suspension, Zoetis, Parsippany-Troy Hills, NJ) (CEFT), (3) enrofloxacin administered subcutaneously in the neck at a dosage of 12.5 mg/kg BW (Baytril 100, Elanco Animal Health, Greenfield, IN) (ENRO), (4) florfenicol administered subcutaneously in the neck at a dosage of 40 mg/kg BW (NUFLOR Injectable Solution, Merck Animal Health, Madison, NJ), (5) oxytetracycline administered subcutaneously in the neck at a dosage of 4.1 mg/kg BW (Noromycin 300 LA, Lenexa, KS) (OXYT), (6) tildipirosin administered subcutaneously in the neck at a dosage of 6.2 mg/kg BW (Zuprevo, Merck Animal Health, Madison, NJ) (TILD), (7) tulathromycin administered subcutaneously in the neck at a dosage of 2.5 mg/kg BW (DRAXXIN Injectable Solution, Zoetis, Parsippany-Troy Hills, NJ) (TULA). All treatments were administered one time per label dosing and administration at day 0, following Beef Quality Assurance guidelines. To minimize interference between treatments, an empty pen was left between treatment groups to eliminate nose-to-nose contact. Following treatment allocation and sampling on day 0, the NC cattle were processed first followed by ENRO, FLOR, TULA, TILD, CEFT, and OXYT every sampling day. The sampling order of treatment groups was consistent throughout this trial. The chute, tub, and holding pens were physically cleaned with soap and brushes, then disinfected with Virkon S (Lanxess AG, Cologne, Germany) per

label instructions between sampling each treatment group across all timepoints following day 0.

2.3. Housing and management

Steers were housed in soil-surfaced pens with 20.8 meters² of space allowance. The linear bunk space per animal was 50.6 centimeters, and the cattle were fed the same starter diet throughout the entire 56-day trial. Cattle were fed once daily at approximately 1,000 h, and feed bunks were visually evaluated twice daily at 0630 and 2,130 h to determine adjustments to feed offering. Feed bunks were managed according to standard operating procedure at the WTAMU Research Feedlot, with a goal of little to no feed remaining at 0630 the following morning. Feed samples were collected twice weekly for dry matter (DM) determination and a diet composite was taken every 2 weeks for nutrient composition analysis at a commercial laboratory (Servi-tech Labs, Amarillo, TX; [Supplementary File S1](#)). Orts were collected, weighed, and analyzed for DM determination in a forced-air oven at 40.5° C for 24 h and used to adjust DM intake.

2.4. Sample collection and RNA extraction

On days 0, 3, 7, 14, 21, and 56, blood samples were collected into PAXgene RNA Blood Tubes (QIAGEN, Germantown, MD) and placed on ice packs at approximately 4° C for transportation to the Texas A&M University Veterinary Education, Research, and Outreach laboratory (Canyon, TX) where they were frozen at -80° C until RNA extractions were performed. From the total pool of 630 samples, a subset ($n = 252$) was selected for RNA extraction and sequencing. For subset selection, six random animals were chosen from each treatment pen over all six timepoints, with the exclusion of sentinel controls due to budgetary constraints. The PAXgene Blood miRNA Kit (QIAGEN, Germantown, MD) was used in conjunction with automated processing *via* a QIACube Connect device (QIAGEN, Germantown, MD) to isolate total RNA from all samples according to manufacturer protocol. Following isolation, RNA quantity (mean RNA yield = 2864.9 ± 1319.5 ng) and quality (mean RIN = 8.4 ± 0.7) were measured *via* a Qubit Flex Fluorometer (Thermo Fisher Scientific, Waltham, MA) and TapeStation 4,200 (Agilent Technologies, Santa Clara, CA), respectively. Complete metadata table, including breed identity based on visual inspection (Btau: *Bos taurus*; Ind: *Bos indicus*), for each individual sample is found in [Supplementary File S2](#).

2.5. RNA sequencing and bioinformatic processing

Library preparation was performed with the Stranded mRNA Library Kit (Illumina, San Diego, CA) per manufacturer's instruction, with 150 bp paired-end sequencing (2×150) performed with a NovaSeq 6,000 S4 v1.7+ (Illumina, San Diego, CA; S4 reagent kit, v1.5) across three lanes at the North Texas Genome Center (NTGC, Arlington, TX); sequencing resulted in a median of 34.1 ± 5.6 M paired-end reads per sample. Following sample demultiplexing *via* bcl2fastq2 v2.20, raw sequenced reads were quality assessed with

FastQC v0.11.9¹ and MultiQC v1.12 (17). Reads were subsequently trimmed for ambiguous base calling, retained Illumina adaptors, and minimum read lengths with Trimmomatic v0.39 (18) (mean retainment: 99.486%; $\sigma = 0.003\%$) using the following parameters: “ILLUMINACLIP:TruSeq3.fa:2:30:10:2:TRUE,” “SLIDINGWINDOW:4:20,” “MINLEN:28,” “LEADING:3,” and “TRAILING:3.” Following read quality assessment and trimming, retained trimmed reads were mapped and indexed to the *Bos taurus* reference assembly ARS-UCD1.3 via HISAT2 v2.21 (19) with default parameters. Sequence Alignment Map (.sam) files generated from HISAT2 alignments were converted to Binary Alignment Map (.bam) files via Samtools v1.14 (20), with default parameters, prior to transcript assembly. Transcript assembly and relative gene-level expression estimation was performed via StringTie2 v2.2.0 (21), with default parameters and workflow described by Pertea and colleagues (22). Following merged Gene Transfer Format (.gtf) file generation of expression estimates for each sample, post-processing for the appending of ambiguous gene-level identifications (“MSTRG” tags) was performed with a custom Perl script provided by Pertea.² Raw gene-level count matrices for each sample were generated with the Python3 script prepDE.py3 (22), selecting for an average read length (“- 1”) of 150 and all other parameters set to default. All raw sequencing data and curated metadata produced by this study are available at the National Center for Biotechnology Information Gene Expression Omnibus (NCBI-GEO) under the accession number GSE225025.

2.6. Differential gene expression analysis

Raw gene counts generated for each sample were processed and analyzed in RStudio v2022.02.3 + 492 with the Bioconductor package edgeR v3.40.2 (23, 24). All analyses were performed as treatment groups versus NC (CEFT vs. NC, ENRO vs. NC, etc.) across all six timepoints. The ComBat_seq function in the sva package v3.46.0 was used to adjust for batch effects, in the form of sequencing lanes, using an empirical Bayes framework in the raw gene counts (25); this was applied to all sequencing libraries at the same time. Raw counts were processed and filtered using the filterByExpr function in the edgeR package as described by Chen et al. (26), utilizing gene counts-per-million (CPM) of 0.2 across a minimum of 12 samples. Library normalization was performed with the trimmed means of M-values method (TMM) (27). Differentially expressed genes (DEGs) were identified through pairwise comparison of NC and each treatment group using likelihood ratio testing (glmLRT) where DEGs were considered significant with a false discovery rate (FDR) of ≤ 0.1 . Specifically, all edgeR analyses were performed within each time point (ex. Day 0, Day 3, etc.) between each treatment group versus the negative control group (ex. CEFT vs. NC, ENRO vs. NC, etc.). The package glmmSeq v0.2.0 was used to investigate changes in gene expression between treatment groups (28). In this generalized linear mixed model, timepoint, group and the interaction of timepoint:group were analyzed as fixed effects with breed and animal

ID included as random effects. Heatmapping was performed using the R package pheatmap v1.0.12,³ utilizing data-centered and normalized z-scores from log2CPM TMM-normalized gene counts; Ward’s minimum variance method was used with calculated Spearman correlation coefficients, further grouped through k-means clustering, and Minkowski distances for clustering dissimilarities by row (gene) and column (sample), respectively. The list of DEGs found in the glmmSeq and edgeR models were compared in Excel, and DEGs identified through group-level comparisons which were shared between the lists at each timepoint were identified using a conditional formatting rule that highlighted duplicate DEGs between the lists of genes from glmmSeq and edgeR. The matching DEGs were then annotated using the National Center for Biotechnology (NCBI) gene database using the bovine and human reference genomes to annotate “LOCI” genes when required. Functional enrichment was performed on the resulting lists of shared DEGs at each timepoint found between the two analyses (glmmSeq and edgeR).

2.7. Downstream analysis of DEGs

Pathway analysis and Gene Ontology (GO) were performed using KOBAS-intelligence v3.0 (29). Overrepresentation analysis used hypergeometric distribution and Fisher’s exact testing to evaluate whether the gene symbols entered were overrepresented in a specific functional gene set. Pathway databases utilized were KEGG and Reactome (30, 31). Benjamini-Hochberg procedure was used for multiple hypothesis correction, and the FDR cutoff for significance was 0.05 (32). GO terms consist of biological processes, molecular functions, and cellular components that the identified DEGs enriched. Specifically, functional enrichment analyses were conducted in two parts for each treatment group: first by DEGs identified through group-level comparisons (i.e., shared genes between glmmSeq (group) and edgeR glmLRT pairwise testing) and, second, by those DEGs identified by glmmSeq timepoint:group interactions. Additionally, principal component analysis (PCA) was conducted with the Bioconductor package PCAtools v2.10.0.⁴ Metadata components for PCA correlational analysis included average daily gain (ADG), animal ID, timepoint of sample collection, and treatment group. Intervene was used to compute pairwise intersections and plot-associated metrics as correlation plots for DEGs of each treatment group at every timepoint (33).

3. Results

3.1. Identification of DEGs

A total of 13,890 uniquely identified genes were differentially expressed across treatment groups and timepoints, 4,602 of which were identified as differentially expressed with both edgeR and glmmSeq (Table 1; Supplementary File S3). A heatmap was generated to visualize expression patterns across all 252 samples (Figure 1).

1 <https://www.bioinformatics.babraham.ac.uk/projects/fastqc/>

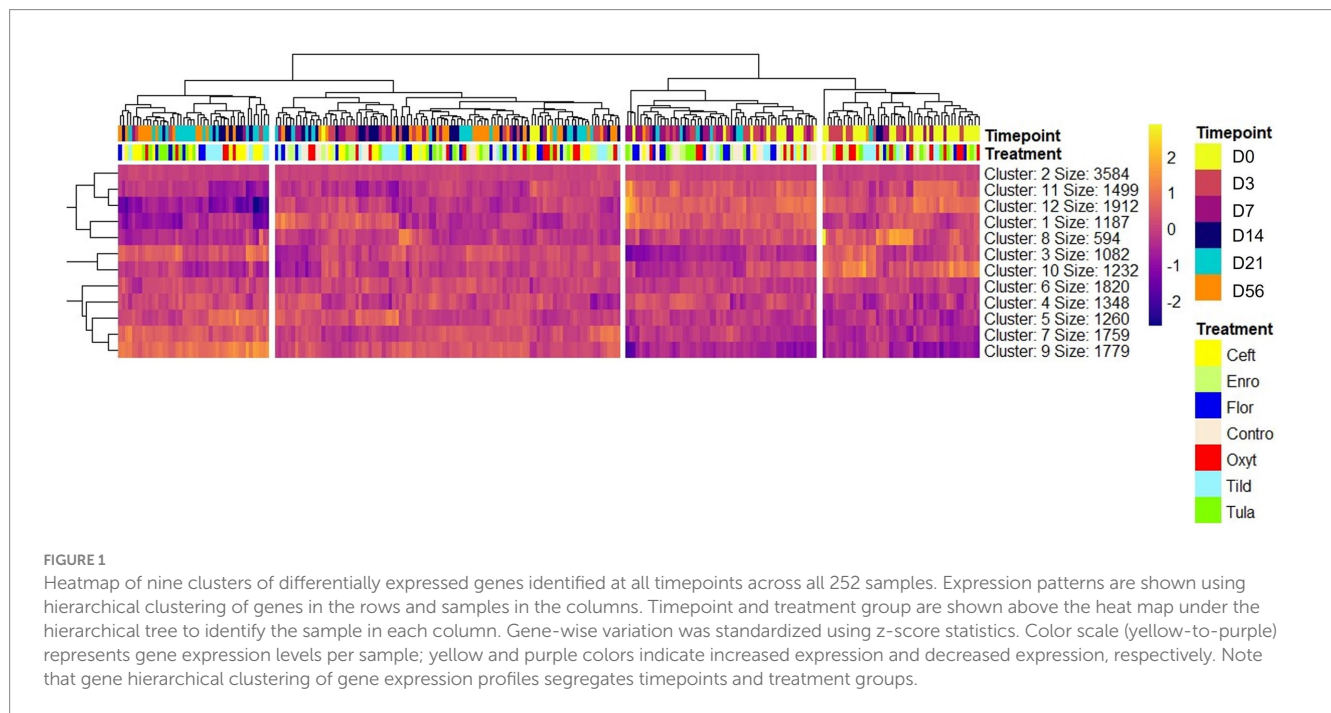
2 <https://gist.github.com/gperta/b83f1b32435e166afa92a2d388527f4b>

3 <https://cran.r-project.org/package=pheatmap>

4 <https://github.com/kevinblighe/PCAtools>

TABLE 1 Number of DEGs identified for each treatment group at each timepoint.

Timepoint	CEFT	ENRO	FLOR	OXYT	TILD	TULA
Day 3	411	58	28	93	1,074	0
Day 7	33	301	8	10	86	1
Day 14	29	2	7	1	116	32
Day 21	104	1	5	3	2,107	63
Day 56	1	2	3	9	13	1



Hierarchical clustering of samples based on expression patterns of DEGs clustered samples by timepoints with days 0, 3, and 7 as the most similar on the right and days 14, 21, and 56 grouping on the left of the map. There was no clear hierarchical clustering of treatment groups.

3.2. Principal component analysis

Using the Elbow method and Horn's parallel analysis (34, 35), the first 12 principal components were chosen, accounting for 47% of the variance in the data as seen in Figure 2. The first principal component (PC) explained 17.9% of the variance and included the strongest and most significant correlation, which was with time ($r=0.67$, $FDR<0.01$) as shown in the Eigencorplot (Figure 3). PC2, which accounted for 6.14% of variance, was negatively correlated with time ($r=-0.16$, $FDR<0.05$). Additionally, PC3 and PC5 were correlated with time as well, but in opposite directions ($r=0.22$, $r=-0.24$, $FDR<0.01$, respectively). The only PCs significantly and negatively correlated to treatment groups were PC11 ($r=-0.31$, $FDR<0.01$) and PC12 ($r=-0.4$, $FDR<0.01$), respectively. These two PCs were also the only components with correlations with animal ID ($r=-0.16$, $r=-0.38$, $FDR<0.05$). A biplot of time across all 252 samples demonstrated the clustering of samples by timepoint as seen by the ellipses in Figure 4.

3.3. Pairwise intersections

Pair-wise intersections of the number of DEGs shared between pairs of antimicrobial treatments at each timepoint, excluding day 0, are shown in Figure 5. There was no shared gene expression between any paired treatment combinations at day 14, day 21, and day 56. At day 3, there were minimal similarities in gene expression shared between tildipirosin and ceftiofur with between 107 and 214 DEGs shared (Supplementary File S3).

3.4. Gene ontology and pathway enrichment analyses

When compared only to NC, unique DEGs were identified for CEFT ($n=526$), ENRO ($n=340$), FLOR ($n=56$), OXYT ($n=111$), TILD ($n=3,001$), and TULA ($n=87$). At day 0, there were no identifiable functional enrichment terms (Tables 2, 3). At day 3, in comparison to NC, there were 44 pathways and 49 GO terms that were enriched for CEFT DEGs ($n=411$). For ENRO, 58 DEGs enriched for two pathways and six GO terms at day 3. There were 28 unique DEGs for FLOR that did not enrich any pathways or GO terms at day 3. For OXYT, 93 DEGs were identified with 67 pathways and 33 GO terms enriched. With the greatest number of

DEGs identified overall, there were 1,074 unique DEGs identified for TILD with a total of 146 pathways and 170 GO terms enriched at day 3. There were no DEGs found for TULA shared between edgeR and glmmSeq analyses at day 3. CEFT, TILD, and OXYT shared multiple functional enrichment pathways related to FcεRI-mediated NF-κB activation and T-cell receptor signaling, which were downregulated in these three treatment groups compared to NC at day 3 as seen in Figures 6, 7, respectively. For the latter pathway, CEFT shared genes with OXYT and TILD that were downregulated which included *RPS27A* and *TAB2*, respectively. Genes uniquely identified for CEFT for T-cell receptor signaling included *TAB2*, *RPS27A*, *ITK*, *MALT1*, and *SKP1*. For this pathway, OXYT had two genes matching CEFT's of the five that were downregulated: *ITK*, *RPS27A*, *PRKCQ*, *ZAP70*, and *CD3G*. Genes downregulated in the TILD cattle included *TAB2*, *NFKBIA*, *CUL1*, *CHUK*, *PAG1*, *BCL10*, and *NCK1*. OXYT and TILD shared one gene, *NFATC2*, related to Th17 cell differentiation at day 3 as seen in Figure 8. Complete findings of functional enrichment analyses at day 3 are found in Supplementary File S4.

In comparison to NC cattle at day 7, CEFT had 33 DEGs that enriched 31 pathways and seven GO terms. With the greatest number of DEGs identified at this timepoint, ENRO had 301 unique DEGs with 42 pathways and 116 GO terms enhanced. There was a decrease in DEGs in FLOR with eight uniquely identified genes that enriched six pathways and 100 GO terms. Similarly, OXYT had 10 DEGs that enriched six pathways and only 24 terms at day 7. For TILD, 86 DEGs were found that enriched nine pathways and one GO term, which was the positive regulation of T-cell apoptotic process. There were not enough DEGs ($n=1$) shared between edgeR and glmmSeq results to perform functional enrichment on TULA at day 7. At this timepoint, ENRO and CEFT enriched for Class I major histocompatibility complex (MHC) mediated antigen processing and presentation pathways (Figure 9), while CEFT and FLOR had DEGs that affected IL-17 signaling pathways (Figure 10). For the pathway related to Class I MHC, DEGs identified for CEFT, *FBXO9* and *SKP1*, were downregulated while DEGs for ENRO (*TRIP12*, *HECTD1*, *ASB7*, *KLHL42*, *HERC3*, *RNF6*, and *CUL1*) were upregulated. Similarly, DEGs for CEFT were downregulated compared to upregulated DEGs for FLOR related to an IL-17 signaling pathway. CEFT genes included *CXCL8* and *TNFAIP3*, and one DEG was identified for FLOR in relation to this pathway, *CEBPB*. Complete findings of functional enrichment analyses at day 7 are found in Supplementary File S5.

At day 14, there were 29 unique DEGs identified for CEFT with seven and 15 pathways and GO terms enriched, respectively. There were not enough DEGs ($n=2$) shared between edgeR and glmmSeq analyses for ENRO at day 14 to perform functional enrichment. For FLOR, seven DEGs that enriched for seven pathways and 83 GO terms were identified. There were not enough DEGs ($n=1$) identified at day 14 for OXYT to perform functional enrichment. TILD had 116 unique DEGs that enriched four pathways and five GO terms at this timepoint. For TULA, 32 DEGs were identified, and the most pathways at 232 and 86 terms were enriched. No shared pathways between treatments were identified. There were 19 pathways and eight GO terms enriched for TULA related to NF-κB activation, and interleukin and interferon signaling. Three genes were enriched for these pathways and included *RPS27A*, *IFNG*, and *CD48*. See Figure 11.

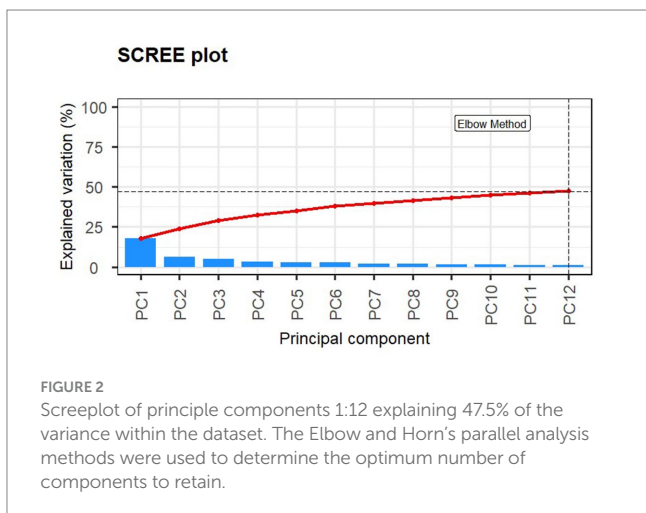


FIGURE 2
Screeplot of principle components 1:12 explaining 47.5% of the variance within the dataset. The Elbow and Horn's parallel analysis methods were used to determine the optimum number of components to retain.

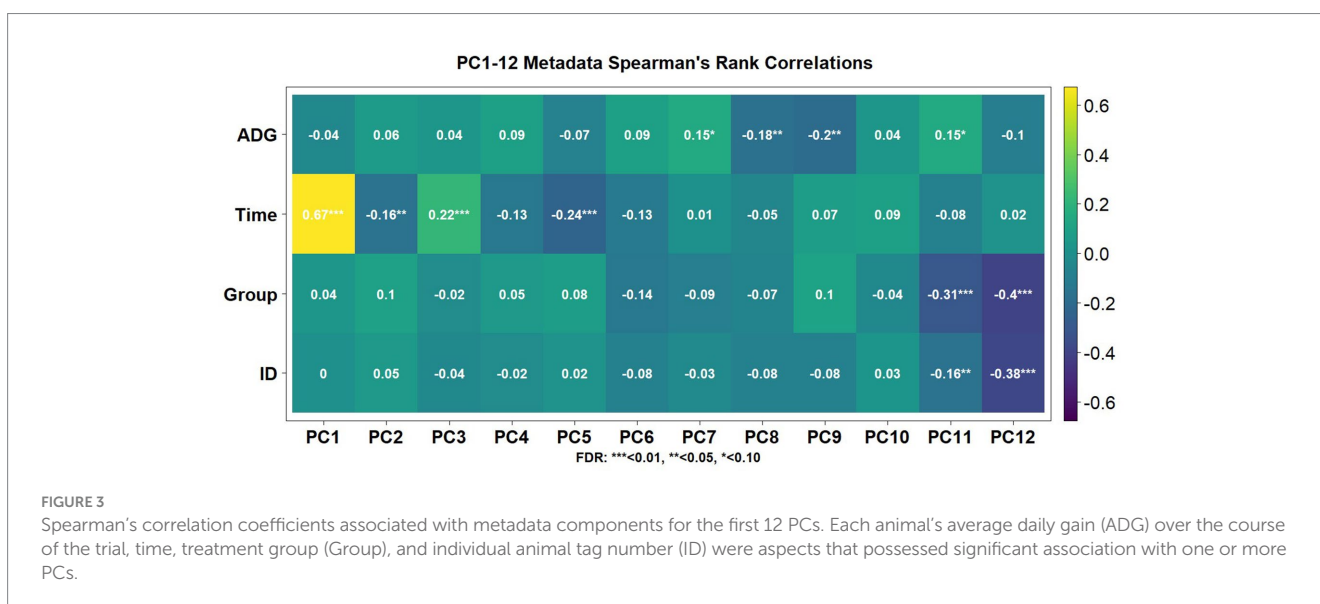


FIGURE 3
Spearman's correlation coefficients associated with metadata components for the first 12 PCs. Each animal's average daily gain (ADG) over the course of the trial, time, treatment group (Group), and individual animal tag number (ID) were aspects that possessed significant association with one or more PCs.

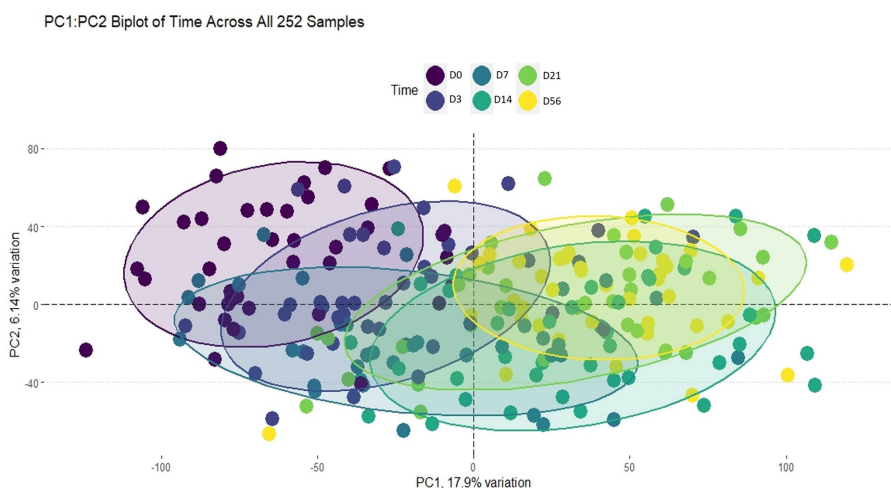


FIGURE 4
Biplot of PC1:PC2 of time across all 252 samples. The ellipses are colored by timepoint as indicated by the legend. Clustering by each timepoint can be seen, indicating time played an important role in explaining the variance within this dataset.

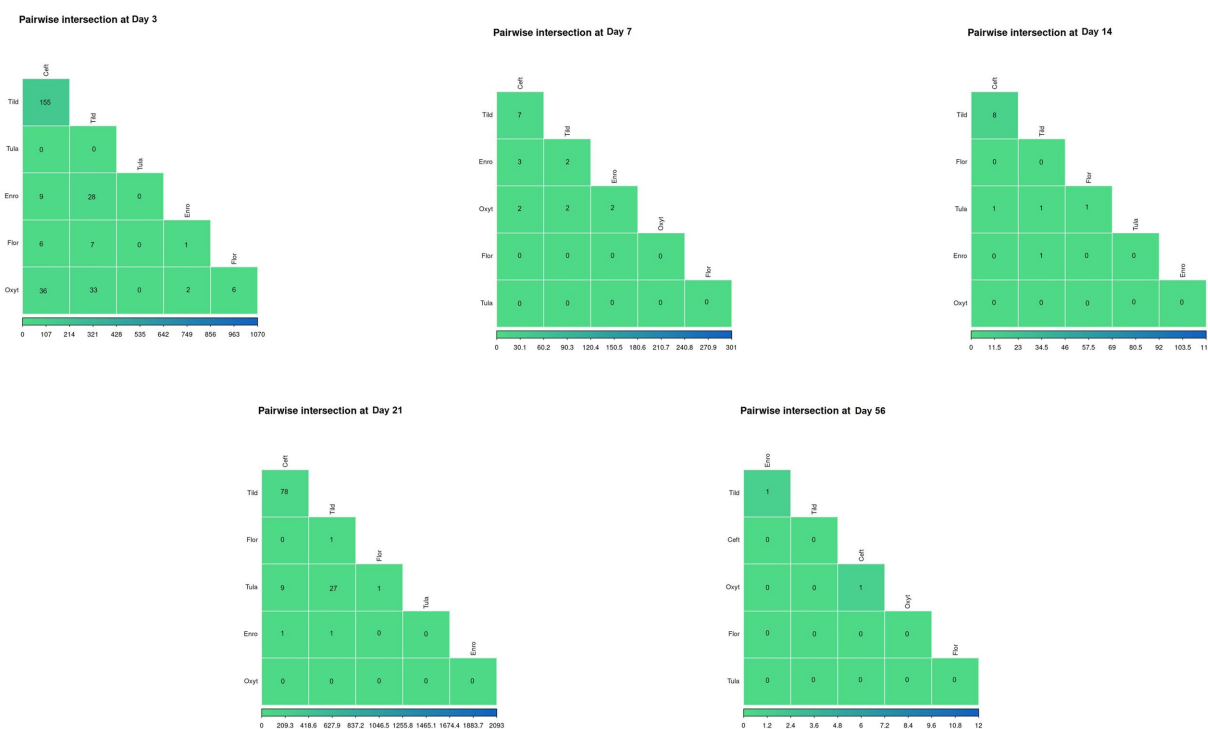


FIGURE 5
Pairwise intersections between the number of DEGs found for every treatment group at each timepoint. Color scale (green-to-blue) shows the number of DEGs in common between treatment groups; green and blue represents decreased number of overlapping DEGs and increased number of overlapping DEGs, respectively.

Complete findings of functional enrichment analyses at day 14 are found in [Supplementary File S6](#).

When compared to NC, 104 unique DEGs were identified for CEFT at day 21, and they enriched for one Reactome pathway and one GO term. There were not enough DEGs ($n = 1$) shared between edgeR and glmmSeq for ENRO at day 21 to perform functional enrichment. FLOR had five DEGs that enriched for 132 pathways and 53 GO terms

at this timepoint. OXYT had three DEGs identified, but they could not be annotated to perform functional enrichment. Once again, with the largest number of DEGs, 2,107 genes were identified for TILD and enriched for 162 pathways and 185 GO terms. TULA had 63 unique DEGs in common between edgeR and glmmSeq that enriched eight pathways and four GO terms. There were no shared pathways between any treatment groups. At day 21, TILD had 13 enriched pathways

TABLE 2 Number of enriched pathways identified for each treatment group at each timepoint.

Timepoint	CEFT	ENRO	FLOR	OXYT	TILD	TULA
Day 3	44	2	0	67	146	0
Day 7	31	42	6	6	9	0
Day 14	7	0	7	0	4	232
Day 21	1	0	132	0	162	8
Day 56	0	0	127	23	9	0

TABLE 3 Number of gene ontology terms identified for each treatment group at each timepoint.

Timepoint	CEFT	ENRO	FLOR	OXYT	TILD	TULA
Day 3	49	6	0	33	170	0
Day 7	7	116	100	24	1	0
Day 14	15	0	83	0	5	86
Day 21	1	0	53	0	185	4
Day 56	0	0	53	35	36	0

related to cytokine signaling in the immune system as shown in Figure 12. Complete findings of functional enrichment analyses at day 21 are found in Supplementary File S7.

At day 56, CEFT and ENRO did not have enough DEGs ($n=1$, $n=2$, respectively) to perform functional enrichment. However, FLOR had three DEGs that enriched for 127 pathways and 53 GO terms. There were nine DEGs for OXYT that enriched 23 pathways and 35 GO terms. For TILD, there were 13 DEGs shared between analyses that coded for nine pathways and 36 GO terms. TULA only had one DEG identified that did not enrich any pathways or terms. There were no specific pathways shared among treatment groups at this timepoint. Complete findings of functional enrichment analyses at day 56 are found in Supplementary File S8.

For timepoint:group interactions, unique DEGs ($FDR \leq 0.05$) were found for CEFT ($n=339$), ENRO ($n=257$), FLOR ($n=319$), OXYT ($n=236$), TILD ($n=373$), and TULA ($n=276$) (Supplementary File S3). Functional enrichment was performed for each timepoint:group comparison. There were 14 pathways and 32 GO terms for CEFT, primarily related to cell scavenging, cell surface activity and reception, ion binding and transport, and sarcomere and myosin activity. For ENRO, there were 6 pathways and 13 GO terms enriched, including the upregulation synthesis of prostaglandins and thromboxanes, chloride and calcium channel/cell membrane activity, and cell membrane synapse and depolarization. For FLOR, there were 2 pathways and 15 GO terms, related to lipopolysaccharide binding, hydrogen peroxide biosynthesis, collagen and intermediate filament organization, and defense against gram-negative bacteria. For OXYT, there was enrichment for only 1 pathway and 3 GO terms, of which were relatively non-specific and unrelated to immunomodulation. For TILD, there were 4 pathways and 14 GO terms enriched, related to the positive regulation of neutrophil chemotaxis, extracellular matrix structure and receptor interaction, and autophagy. For TULA, no pathways were enriched, and there were 11 GO terms, which corresponded with carbohydrate binding, ion transport and binding, extracellular matrix structure, and defense response against gram-positive bacterium. Complete findings of functional enrichment analyses for timepoint:group interactions for all treatments across all timepoints are found in Supplementary File S9.

4. Discussion

Previous research has sufficiently employed the use of transcriptomics and RNA-Seq in the exploration of predictive biomarkers for BRD, the pathogens involved in development of this disease, and the presence of antimicrobial resistance genes (ARGs) of the bacterial pathogens associated with BRD. Trials utilizing tissue samples such as lung, lymph nodes, and tonsils have demonstrated how each viral and bacterial agent acts as a pathogen, causing clinical disease (11, 12). More recently, the whole blood transcriptome has been investigated for potential predictive molecules, protective immunological mechanisms, and regulatory patterns of BRD in beef cattle (13, 14, 36, 37). Whole genome sequencing has also been used to examine bacterial transcriptome profiles and identify ARGs and the drug classifications of which species have developed resistance (10, 38, 39). Although the findings mentioned above are pertinent to attempt to understand BRD and involved pathogens, there is a lack of transcriptome research examining the relationship between antimicrobials and their effects on the host immunological response. Identifying mechanisms and potential secondary properties of antimicrobials is important to understanding how drugs maintain efficacy despite the rise of AMR.

In this study, we identified 34,267 DEGs associated by day (i.e., time) and 1,800 DEGs associated with the interaction of group and day in glmSeq (Supplementary File S3). Based on hierarchical clustering of total gene expression across all samples (Figure 1), time was a major component in driving discernible gene expression patterns; days 0, 3 and 7 clustered while days 14, 21, and 56 shared more similar gene expression patterns. The biplot of PC1:PC2 also demonstrated the importance of time within this dataset as seen by the clustering of the ellipses by timepoint (Figure 4). Time is shown to biologically factor in the development of the immune system, where progression of the immune systems in calves occurs in small steps from conception to maturity at approximately 6 months after birth (40). The cells associated with innate immunity, such as neutrophils, macrophages, and natural killer cells, are influenced by age and time. While neutrophil counts may be higher in neonatal calves, their phagocytic abilities are reduced compared to older calves, as are

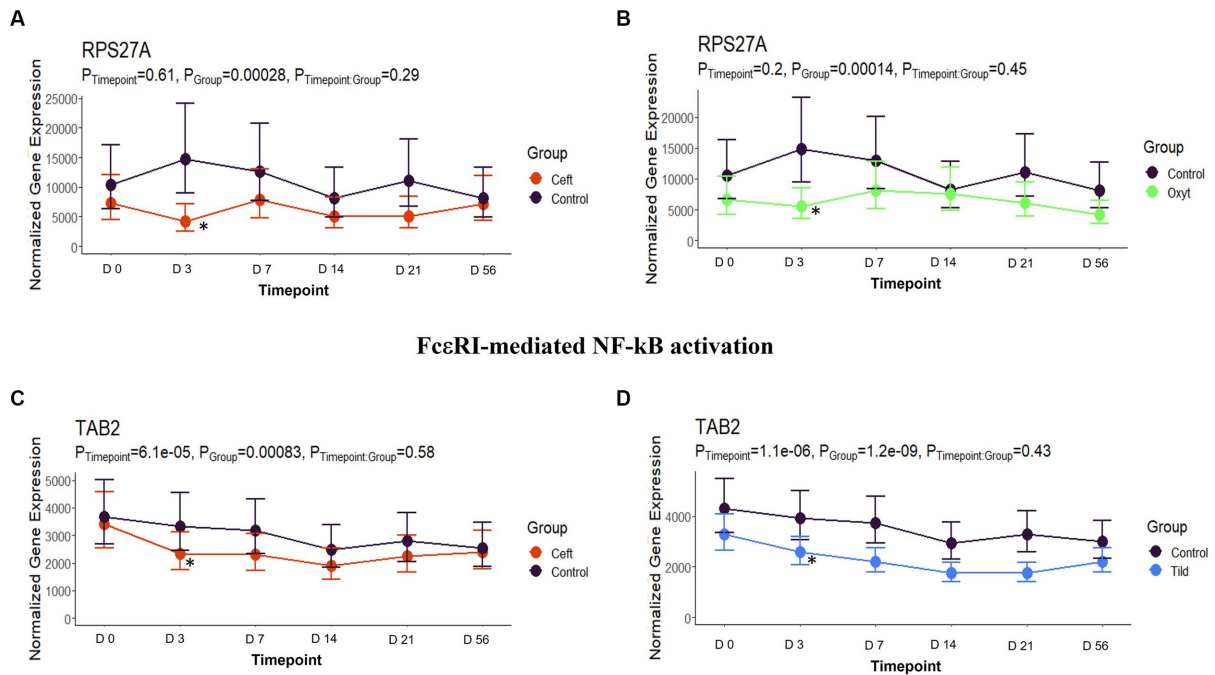


FIGURE 6

FcεRI-mediated NF-κB activation gene expression for CEFT, OXYT, and TILD. (A) Trended normalized averages calculated from \log_{10} transformed gene expression over time of *RPS27A* for CEFT. (B) Trended normalized averages calculated from \log_{10} transformed gene expression over time of *RPS27A* for OXYT. (C) Trended normalized averages calculated from \log_{10} transformed gene expression over time of *TAB2* for CEFT. (D) Trended normalized averages calculated from \log_{10} transformed gene expression over time of *TAB2* for TILD. The dots represent the average gene expression level at that timepoint, and the bars represent the standard error of gene expression found at each timepoint in each group. NC is represented by the black lines.

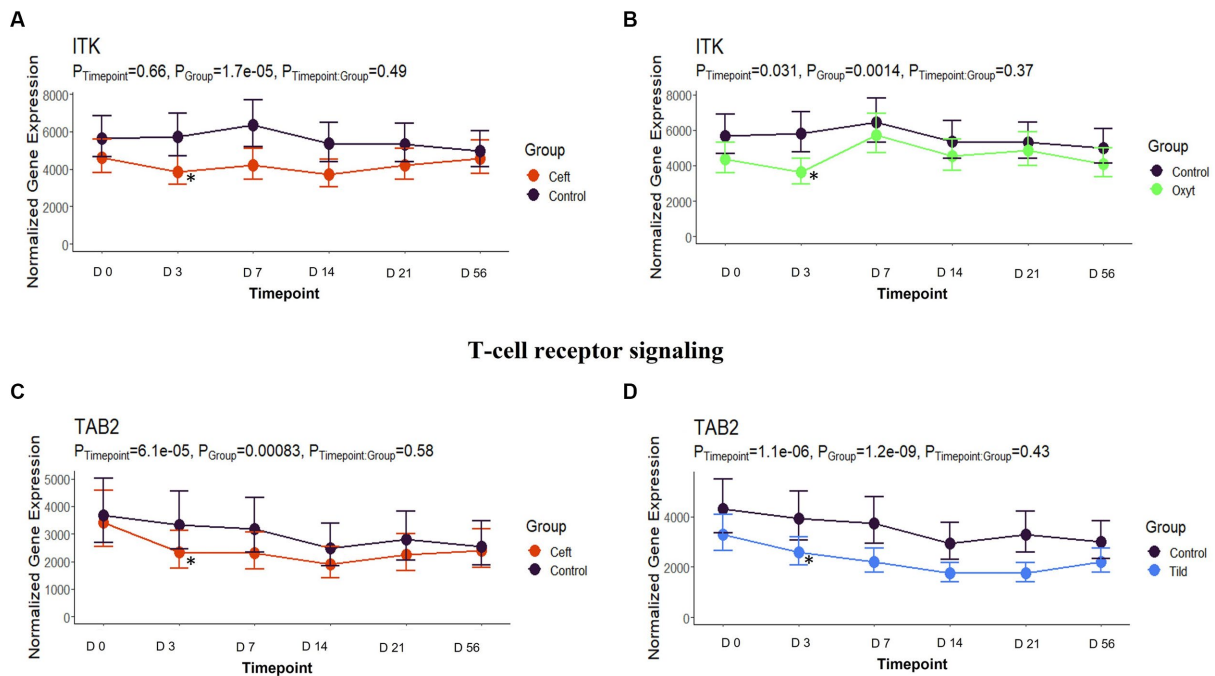
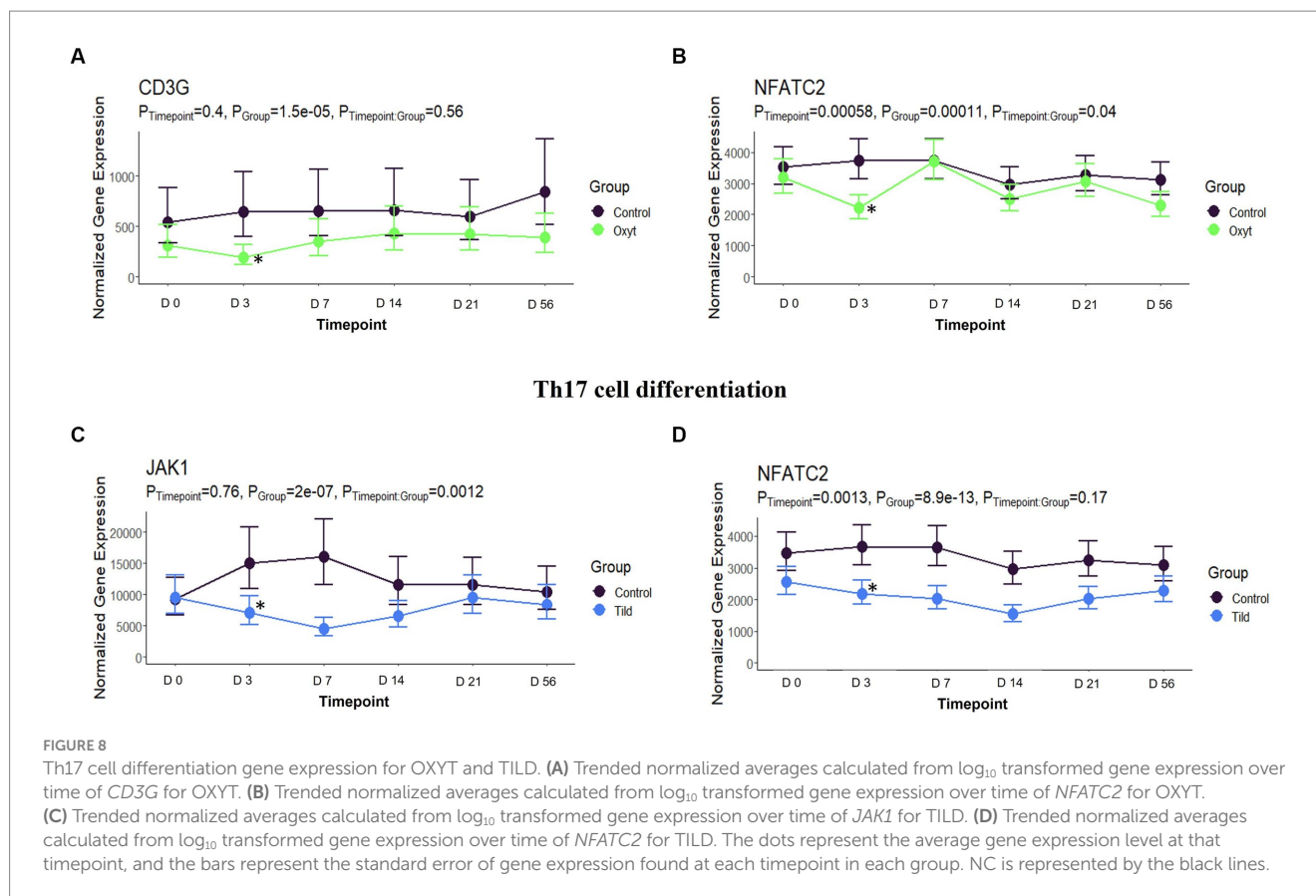


FIGURE 7

T-cell receptor signaling gene expression for CEFT, OXYT, and TILD. (A) Trended normalized averages calculated from \log_{10} transformed gene expression over time of *ITK* for CEFT. (B) Trended normalized averages calculated from \log_{10} transformed gene expression over time of *ITK* for OXYT. (C) Trended normalized averages calculated from \log_{10} transformed gene expression over time of *TAB2* for CEFT. (D) Trended normalized averages calculated from \log_{10} transformed gene expression over time of *TAB2* for TILD. The dots represent the average gene expression level at that timepoint, and the bars represent the standard error of gene expression found at each timepoint in each group. NC is represented by the black lines.

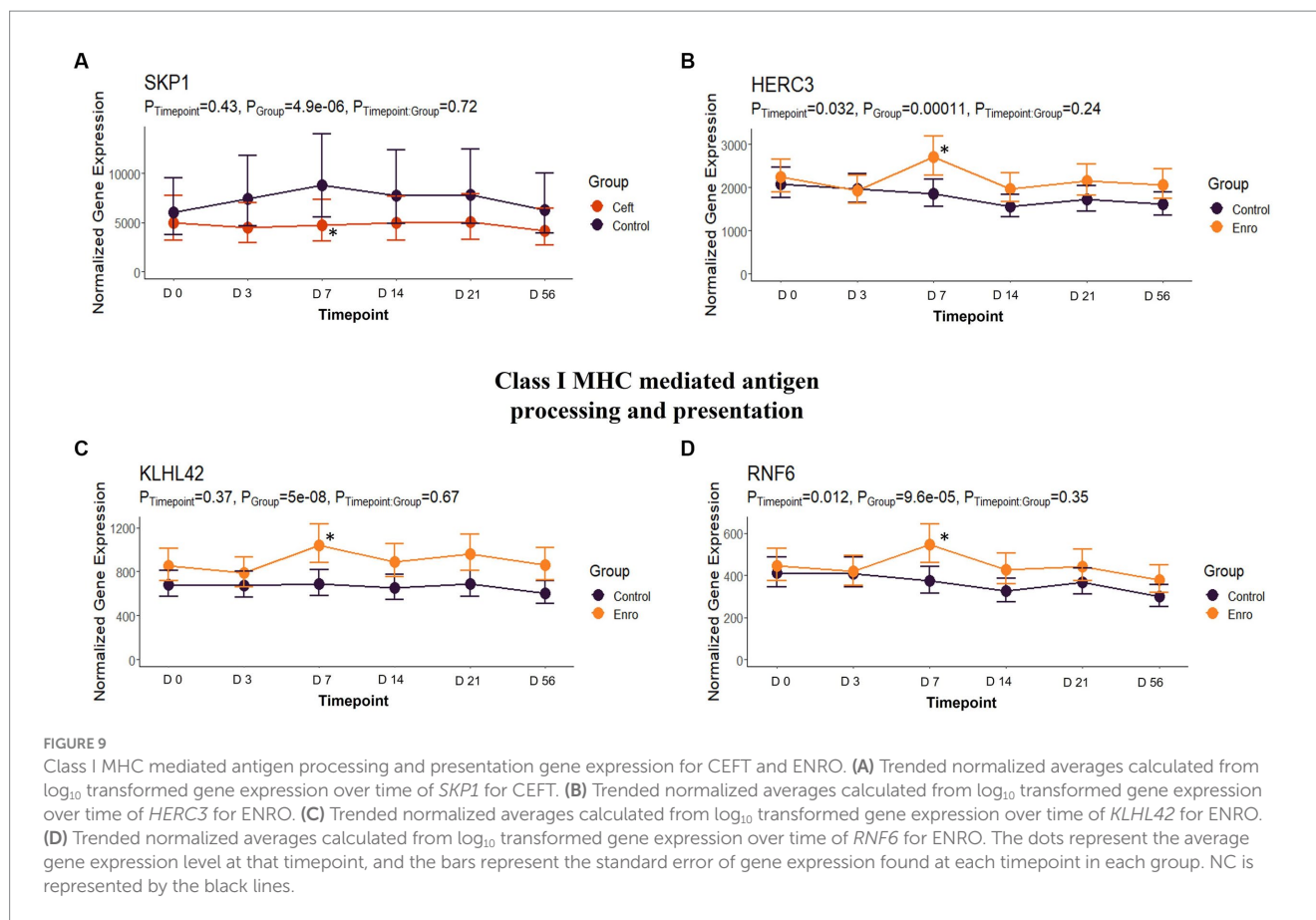


macrophages (41). Neutrophil activity increases to adult levels by 5 months of age (40). When calves enter feedlots at lower weights and younger ages, they are predisposed to BRD, largely due to the fact their immune system is not always fully developed. In cattle, most of the immune system maturity is seen between five and 8 months of age. While this does not mean that young calves are not capable of responding to antigens, the response may be weaker and thus, easier for pathogens to overcome (42). With the addition of novel pathogens, their immune systems fail to produce a sufficient response to protect them from developing BRD upon arrival to a stocker or feedlot facility (42). Previous research suggests that peak clinical signs of disease occur 7 to 14 days after peak exposure to viral and bacterial pathogens (3, 43, 44). There are other factors that potentially explain the effect time had on this dataset, such as physiological stress and acclimation. The effect physiological stress can have on a calf's immune system can lead to prolonged activation of the hypothalamus-pituitary-adrenal (HPA) axis, suppressing the immune system and increasing susceptibility to disease (45). Additionally, acclimation to a new environment and exposure to novel pathogens is a hypothesis to consider. In response to this acclimation, many calves' immune systems are unable to mount an appropriate response. Therefore, time plays an important role in host immunological response to antimicrobials administered metaphylactically.

In the present study, we identified 4,602 DEGs across the six antimicrobials administered (Supplementary File S3; Table 1). Regarding functional enrichment of these DEGs (Supplementary Files S4–S8), the major functions found across treatments included cytokine signaling and T-cell receptor signaling

pathways. There was no hierarchical clustering by treatment group (Figure 1) and no correlations between groups as shown by the pairwise intersection plots (Figure 5), suggesting each antimicrobial acts through various mechanisms controlled by different DEGs. At day 3, FcεRI-mediated NF-κβ activation pathways were enriched for CEFT, OXYT, and TILD. As supported by previous literature, ceftiofur and oxytetracycline inhibited NF-κβ activation by reducing the translocation of NF-κβ from the cytoplasm to the nucleus and *via* phosphorylation, respectively (46, 47). CEFT and OXYT had one DEG in common to regulate this pathway even though they affect NF-κβ through different mechanisms: *RPS27A*. To our knowledge, there is no published literature regarding tildipirosin's downregulation of FcεRI-mediated NF-κβ activation. However, clarithromycin has been reported to inhibit NF-κβ activation in human peripheral blood mononuclear cells and pulmonary epithelial cells (48). TILD and CEFT share a DEG (*TAB2*) that enriches this pathway (Figure 6). It is inappropriate to assume that they use the same mechanism though due to the lack of published literature regarding tildipirosin's effect on FcεRI-mediated NF-κβ activation.

Downregulation of T-cell receptor signaling also occurred at day 3 by CEFT, OXYT, and TILD. The influence of ceftiofur on T-cells and B-cells has been investigated in chicks, and it was found that the percentages of both types of cells were decreased (49). A change in the specific T-cell type ratio was also observed with decreased percentages of CD4⁺ CD8⁻ cells (49). A study conducted by Platania et al. (50) demonstrated that oxytetracycline reduced the proliferative response of T lymphocytes through an *in vivo* model of autoimmune disease related to glucocorticoid-induced tumor necrosis factor



receptor-related gene (*GITR*; *TNFSRF18*) in mice. While tildipirosin was not specifically mentioned, another macrolide (rapamycin) was reported to interfere with signal transduction pathways required for T-cell activation and growth in various species such as mice, pigs, and monkeys (50). The inhibitory effects of rapamycin on T-cell activation were mediated through the formation of pharmacologically active complexes with members of a family of intracellular receptors that are signaling proteins required for T-cell antigen receptor engagement (50).

The final pathway enriched among multiple treatments at day 3 is related to T-helper (Th) 17 cell differentiation. *OXYT* and *TILD* have one DEG in common for this pathway out of four and seven genes, respectively (*NFATC2*). While, to our knowledge, there is no published literature regarding oxytetracycline and Th17 cell differentiation, there has been a report of another tetracycline: minocycline. Minocycline treatment in mice reduced the production of interleukin (IL)-17, and a positive correlation between glucocorticoid-induced tumor necrosis factor receptor-related gene (*GITRL*) signaling and Th17 induction has been reported in previous literature (51, 52). Tang and colleagues (52) demonstrated that IL-17 production and Th17 differentiation was triggered by *GITLR* intracellular signaling. Similarly, there was no previous research for tildipirosin's effect on Th17 differentiation. However, clarithromycin, another macrolide, was investigated when treating mice infected with macrolide antibiotic-resistant *Streptococcus pneumoniae* (53). Clarithromycin administration impaired the frequency and number of Th17 cells within the lungs of infected mice. Although the cattle treated in the current trial were healthy, metaphylaxis is applied to

cattle at high risk of developing BRD. Therefore, previous literature investigating antimicrobials and their interactions with bacterial or viral pathogens is highly relevant to understand the importance of mechanisms found by this study.

Class I MHC mediated antigen processing and presentation was a pathway enriched by CEFT and ENRO on day 7, but the drugs regulated the DEGs in opposite directions. Ceftiofur downregulated two genes while enrofloxacin upregulated seven. Another third-generation cephalosporin, ceftriaxone, has been reported to affect antigen presentation by binding directly to the immunogenic peptide embedded in MHC or to cell surface proteins, preventing necessary processing before the presentation (54, 55). This could potentially be the mechanism behind the downregulation of genes in the CEFT cattle. The genes upregulated by enrofloxacin were all related to ubiquitination and proteasome degradation, which play a central role in generating class I MHC antigens. Intracellular foreign or deviated host proteins are cleaved into peptide fragments so they can be loaded on to class I MHC molecules and presented to cytotoxic T-cells (56).

Similarly, the DEGs enriching the pathway for IL-17 signaling were downregulated in CEFT and upregulated in FLOR cattle. No DEGs were shared between the two independent comparisons, suggesting different genomic processes were in use to regulate IL-17. Interleukin-17 is a key cytokine that links T-cell activation to neutrophil mobilization and activation, and IL-17 mediates innate immunity to pathogens or contribute to the pathogenesis of inflammatory disease (57). In previous literature, cefazolin, a first-generation cephalosporin antibiotic, was shown to interact with IL-15-dependent TNF- α and IL-17 synthesis (58). Cefazolin reduced

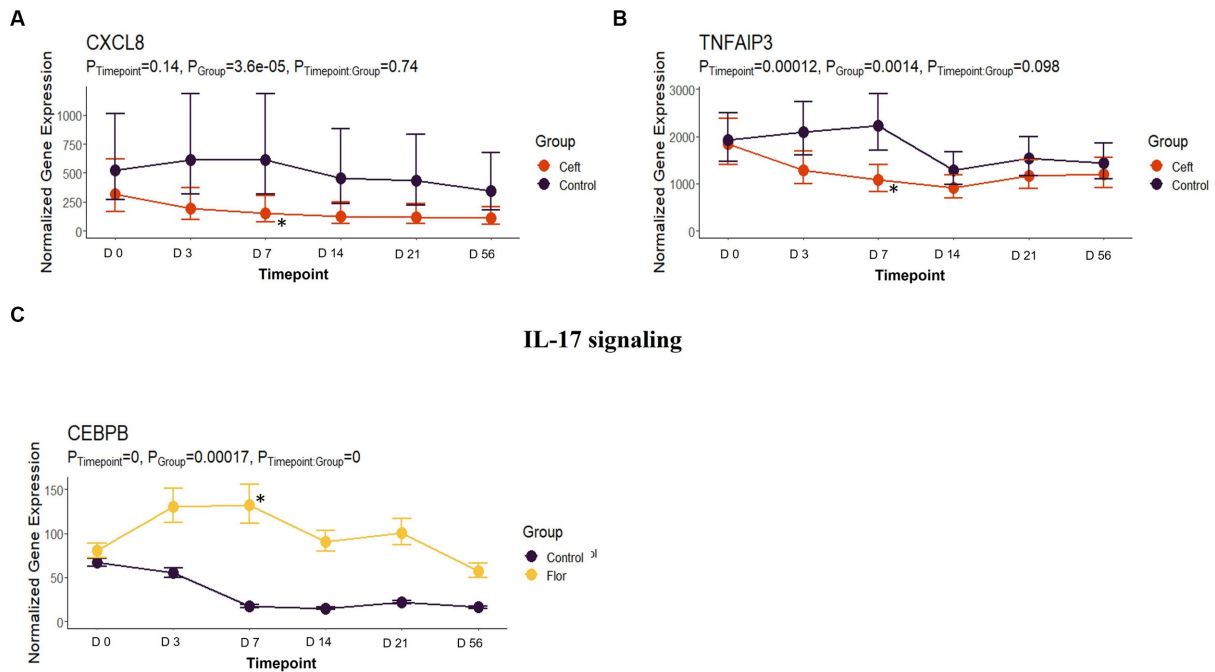


FIGURE 10
 IL-17 signaling gene expression for CEFT and FLOR. **(A)** Trended normalized averages calculated from \log_{10} transformed gene expression over time of *CXCL8* for CEFT. **(B)** Trended normalized averages calculated from \log_{10} transformed gene expression over time of *TNFAIP3* for CEFT. **(C)** Trended normalized averages calculated from \log_{10} transformed gene expression over time of *CEBPB* for FLOR. The dots represent the average gene expression level at that timepoint, and the bars represent the standard error of gene expression found at each timepoint in each group. NC is represented by the black lines.

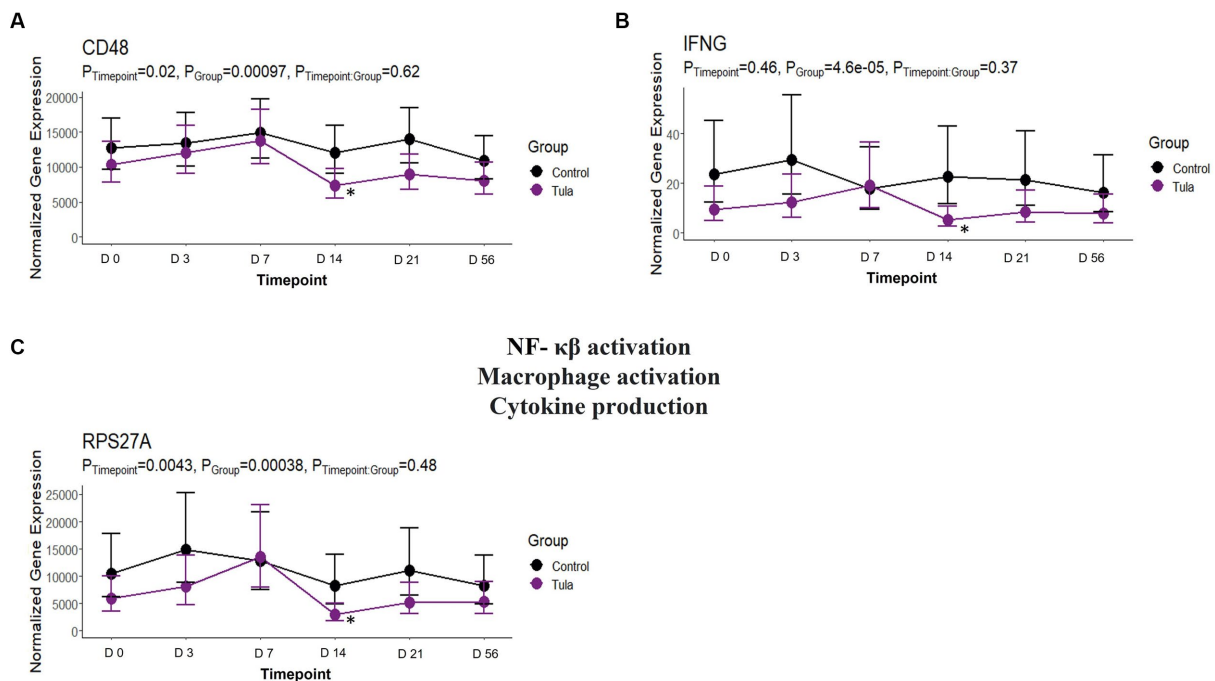
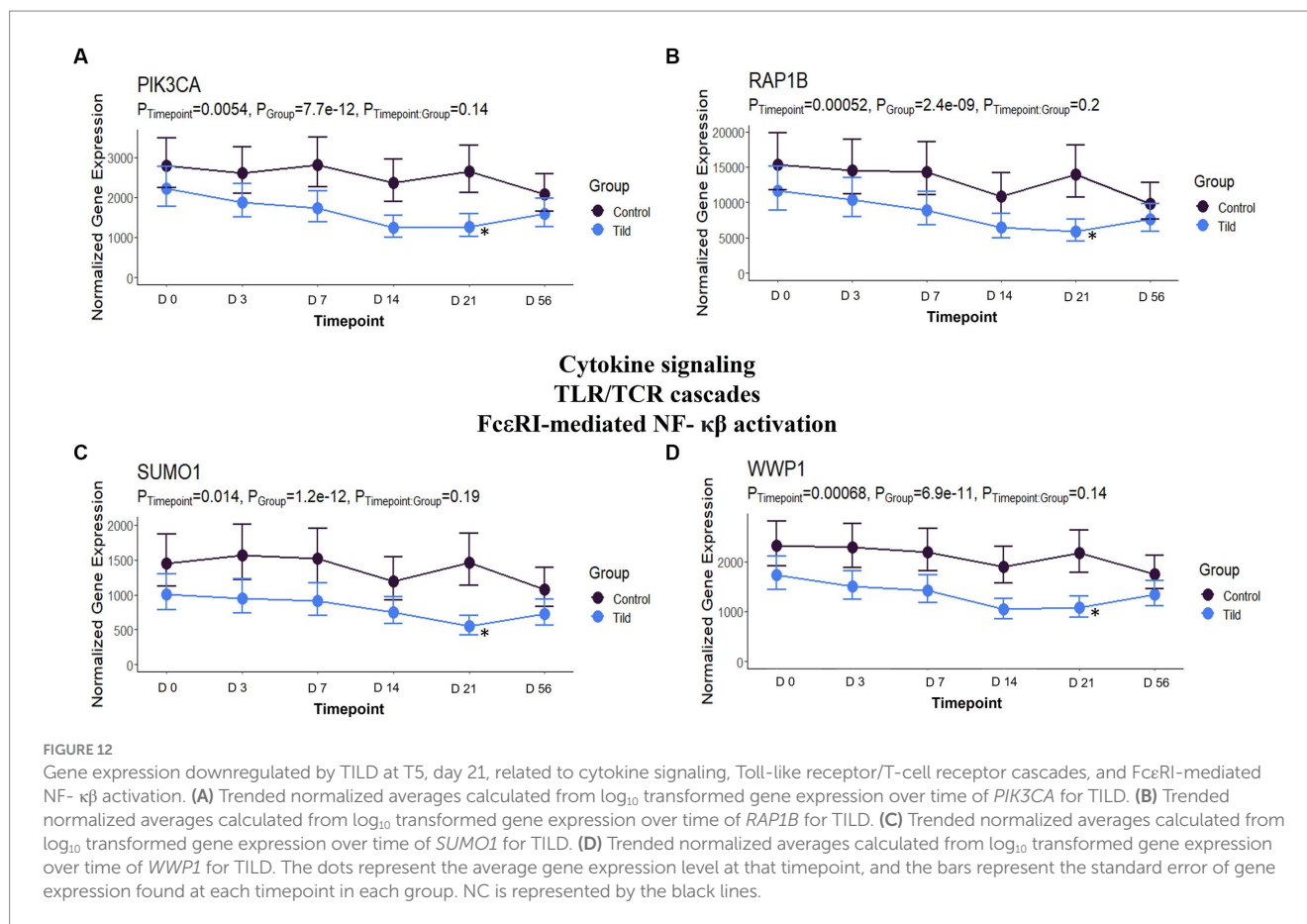


FIGURE 11
 Gene expression downregulated by TULA at T4, day 14, related to NF – κ β activation, macrophage activation, and cytokine production. **(A)** Trended normalized averages calculated from \log_{10} transformed gene expression over time of *CD48* for TULA. **(B)** Trended normalized averages calculated from \log_{10} transformed gene expression over time of *IFNG* for TULA. **(C)** Trended normalized averages calculated from \log_{10} transformed gene expression over time of *RPS27A* for TULA. The dots represent the average gene expression level at that timepoint, and the bars represent the standard error of gene expression found at each timepoint in each group. NC is represented by the black lines.



production of IL-17, among other various cytokines (58). No previous research was identified corroborating the findings of florfenicol's upregulation of *CEBPB* in relation to IL-17, possibly illustrating a novel secondary mechanism for this antimicrobial. The same gene, *CEBPB*, also influenced a tumor necrosis factor (TNF) signaling pathway and a GO term of "positive regulation of inflammatory response."

There were no shared pathways identified at day 14 between any antimicrobials, but TULA possessed 19 pathways and 8 GO terms enriched related to NF-κB activation, macrophage activation and differentiation, and production of various cytokines such as IL-3, IL-5, and IFN-γ. There were three genes acting as the main drivers of the pathways and terms: *RPS27A*, *IFNG*, and *CD48*. It has been reported that tulathromycin significantly inhibits proinflammatory NF-κB signaling in bovine neutrophils and reduced secretion of proinflammatory CXCL-8 in lipopolysaccharide (LPS)-stimulated macrophages (59, 60). In another trial, the effect of tulathromycin was examined in a nonbacterial *in vivo* model of pulmonary inflammation, where tulathromycin administration inhibited phospholipases and altered leukotriene B₄, prostaglandin E₂, and lipoxin A₄ production (61). The findings from the present trial support the anti-inflammatory benefits of tulathromycin while providing insight on the DEGs being downregulated to inhibit pathways discussed above. Furthermore, tulathromycin has been shown to have immunomodulatory effects in species other than cattle, such as rabbits, pigs, and horses (62–64).

On day 21, there were no shared pathways or GO terms between treatment groups. TILD possessed the most DEGs identified, and pathways/GO terms enriched at 2,107 and 347, respectively. Pathways

found were related to cytokine signaling, toll like receptor (TLR)/TCR cascades, and FcεRI-mediated NF-κB activation. Genes downregulating these pathways included *FBX09*, *PIK3CA*, *RAP1B*, *RNF14*, *SUMO1*, *UBE2Q2*, and *WWP1*. Although minimal published literature exists regarding the effect of tildipirosin specifically on cytokines and TCR/TLR cascades, there is evidence that macrolides can interfere with signal transduction of T-cell activation and growth, and the impairment of T-cell production thus decreasing the immune response, shown through trials completed with rapamycin and clarithromycin (50, 53).

On day 56, there were 25 DEGs in total identified across three treatment groups (FLOR, OXYT, and TILD) when compared to NC. However, none of the genes that enriched pathways related to immune function were differentially expressed. This may demonstrate a transient induction or influence of genomic regulation by these drugs, as the majority of the antimicrobials used in this trial possess half-lives less than 3 days, with the exception of tildipirosin which is 9 days in the plasma and 10 days in the lung (65).

To investigate the intersection of time and treatment within this study, we identified several DEGs and functional enrichments within each group comparison. Interestingly, we identified direct immune-related mechanisms in five of the six groups: CEFT, ENRO, FLOR, TILD, and TULA (Supplementary File S9). The GO terms and pathways identified for CEFT primarily related to ion reception and cell scavenging. One study, albeit in combination with vanadium and performed *in vitro*, suggested that cephalosporin interacts with tissue macrophages and act as a reducing scavenger (66). Of particular

interest, DEGs identified within ENRO enriched for prostaglandin and thromboxane syntheses and arachidonic acid metabolism. In recent studies, it has been shown that danofloxacin administration, a closely related fluoroquinolone drug, significantly reduced prostaglandin E2 levels and induced lipid peroxidation (67, 68). From the FLOR enrichment analysis, we identified significant terms and pathways related to lipopolysaccharide (LPS) binding and gram-negative bacterium defense, primarily driven by *LBP*, several members of the cathelicidin family of antimicrobial peptides (*CAMP*, *CATHL1*, and *CATHL2*), and the adhesion G protein-coupled receptor gene *ADGRB1*. Several studies have suggested that florfenicol helps combat bacterial infection, regulate LPS-induced immune proliferation, and quell host inflammation *via* these mechanisms in a concentration-dependent manner (69–72). For both TILD and TULA interaction analyses, we identified enrichment for neutrophil chemotaxis and autophagy, extracellular matrix structure, and defense against bacterium. A recent therapeutic review article related to adjunct therapies for SARS-CoV-2 infection highlights that clinical use of azithromycin, a closely related macrolide, appears to regulate proinflammatory cytokine production, inhibit neutrophilic infiltration, and alters autophagosomes within macrophages (73). While unclear at this time, this may suggest that these macrolides alter neutrophilic release of proinflammatory cytokines, such as IL-1 β , and enhance leukocyte stimulation through autophagy (74, 75).

One limitation of this study was the variation of breeds within the sample population; however, randomization was used to successfully account for this and other potential confounders. Other important confounders such as BW and feed were controlled by the experimental design. This aspect could account for variation biologically between samples. Additionally, there was only one pen per treatment. The lack of replication reduces the ability to extrapolate results to other populations, but these findings provide a direction for further research to explore the mechanisms found for each antimicrobial. A strength of this trial was the detection of DEGs using two different statistical methods, showing the robustness of the results.

Data availability statement

The data presented in the study are deposited in the National Center for Biotechnology Information Gene Expression Omnibus (NCBI-GEO), accession number GSE225025. R code for statistical analyses of raw gene count data is found at <https://github.com/mscott16/metamultiome>.

Ethics statement

The animal study was approved by West Texas A&M University (WTAMU) Institutional Animal Care and Use Committee. The study was conducted in accordance with the local legislation and institutional requirements.

Author contributions

RB: Data curation, Formal analysis, Investigation, Methodology, Validation, Visualization, Writing – original draft, Writing – review & editing. JR: Conceptualization, Funding acquisition, Investigation,

Methodology, Project administration, Resources, Supervision, Validation, Writing – review & editing. MM: Data curation, Investigation, Methodology, Writing – review & editing. RV-C: Conceptualization, Data curation, Formal analysis, Funding acquisition, Investigation, Methodology, Project administration, Resources, Supervision, Writing – review & editing. PM: Conceptualization, Funding acquisition, Investigation, Methodology, Project administration, Resources, Supervision, Writing – review & editing. JF: Investigation, Methodology, Project administration, Supervision, Writing – review & editing. MS: Conceptualization, Data curation, Formal analysis, Funding acquisition, Investigation, Methodology, Project administration, Resources, Software, Supervision, Validation, Visualization, Writing – review & editing.

Funding

The author(s) declare financial support was received for the research, authorship, and/or publication of this article. This study was internally funded in part by Texas A&M University, School of Veterinary Medicine and Biomedical Sciences and West Texas A&M University, Department of Agricultural Sciences. Additionally, this study was externally funded in part by the Texas Cattle Feeders Association (TCFA).

Acknowledgments

The authors would like to thank the staff at the West Texas A&M University Research Feedlot (Fil Polanco, Daniel Young, Anna Kobza, Parker Dettle) for animal caretaking and sampling. The authors also thank the student staff support at the Texas A&M VERO Research Laboratory (Nerissa Bechtol-Wuest, Maggie Murphy, Max Chung, Chris Panaretos, Dana Burk, Rachel Huff, Cory Wolfe). Additionally, the authors would also like to thank the North Texas Genome Center (NTGC), including Dr. Zibiao Guo.

Conflict of interest

The authors declare that the research was conducted in the absence of any commercial or financial relationships that could be construed as a potential conflict of interest.

Publisher's note

All claims expressed in this article are solely those of the authors and do not necessarily represent those of their affiliated organizations, or those of the publisher, the editors and the reviewers. Any product that may be evaluated in this article, or claim that may be made by its manufacturer, is not guaranteed or endorsed by the publisher.

Supplementary material

The Supplementary material for this article can be found online at: <https://www.frontiersin.org/articles/10.3389/fvets.2023.1272940/full#supplementary-material>

References

- Snyder E, Credille B. Mannheimia haemolytica and Pasteurella multocida in bovine respiratory disease: how are they changing in response to efforts to control them? *Vet Clin North Am Food Anim Pract.* (2020) 36:253–68. doi: 10.1016/j.cvfa.2020.02.001
- Edwards A. Respiratory diseases of feedlot cattle in Central USA. *Bov Pract (Stillwater).* (1996) 30:5–7. doi: 10.21423/bovine-vol1996no30p5-7
- Taylor JD, Fulton RW, Lehenbauer TW, Step DL, Confer AW. The epidemiology of bovine respiratory disease: what is the evidence for predisposing factors? *Can Vet J.* (2010) 51:1095–102.
- Gershwin LJ. Bovine respiratory syncytial virus infection: Immunopathogenic mechanisms. *Anim Health Res Rev.* (2007) 8:207–13. doi: 10.1017/S1466252307001405
- Timsit E, Dendukuri N, Schiller I, Buczinski S. Diagnostic accuracy of clinical illness for bovine respiratory disease (BRD) diagnosis in beef cattle placed in feedlots: a systematic literature review and hierarchical Bayesian latent-class meta-analysis. *Prev Vet Med.* (2016) 135:67–73. doi: 10.1016/j.prevetmed.2016.11.006
- Blakebrough-Hall C, Dona A, D'occhio MJ, McMeniman J, González LA. Diagnosis of bovine respiratory disease in feedlot cattle using blood 1H NMR metabolomics. *Sci Rep.* (2020) 10:115. doi: 10.1038/s41598-019-56809-w
- Ives SE, Richeson JT. Use of antimicrobial Metaphylaxis for the control of bovine respiratory disease in high-risk cattle. *Vet Clin North Am Food Anim Pract.* (2015) 31:341–50. doi: 10.1016/j.cvfa.2015.05.008
- Hampton T. Medical News & Perspectives Report Reveals Scope of US antibiotic resistance threat. *JAMA.* (2013) 310:1661–3. doi: 10.1001/jama.2013.280695
- Wang Z, Gerstein M, Snyder M. RNA-Seq: a revolutionary tool for transcriptomics. *Nat Rev Genet.* (2009) 10:57–63. doi: 10.1038/nrg2484
- Khaledi A, Schniederjans M, Pohl S, Rainer R, Bodenhofer U, Xia B, et al. Transcriptome profiling of antimicrobial resistance in *Pseudomonas aeruginosa*. *Antimicrob Agents Chemother.* (2016) 60:4722–33. doi: 10.1128/AAC.00075-16
- Johnston D, Earley B, McCabe MS, Lemon K, Duffy C, McMenamy M, et al. Experimental challenge with bovine respiratory syncytial virus in dairy calves: bronchial lymph node transcriptome response. *Sci Rep.* (2019) 9:14736. doi: 10.1038/s41598-019-51094-z
- Behura SK, Tizoto PC, Kim J, Grupioni NV, Seabury CM, Schnabel RD, et al. Tissue tropism in host transcriptional response to members of the bovine respiratory disease complex. *Sci Rep.* (2017) 7:17938. doi: 10.1038/s41598-017-18205-0
- Jimenez J, Timsit E, Orsel K, van der Meer F, Guan LL, Plastow G. Whole-blood transcriptome analysis of feedlot cattle with and without bovine respiratory disease. *Front Genet.* (2021) 12:12. doi: 10.3389/fgene.2021.627623
- Sun HZ, Srithayakumar V, Jimenez J, Jin W, Hosseini A, Raszek M, et al. Longitudinal blood transcriptomic analysis to identify molecular regulatory patterns of bovine respiratory disease in beef cattle. *Genomics.* (2020) 112:3968–77. doi: 10.1016/j.ygeno.2020.07.014
- Scott MA, Woolums AR, Swiderski CE, Perkins AD, Nanduri B, Smith DR, et al. Multipopulation transcriptome analysis of post-weaned beef cattle at arrival further validates candidate biomarkers for predicting clinical bovine respiratory disease. *Sci Rep.* (2021) 11:23877. doi: 10.1038/s41598-021-03355-z
- du Sert NP, Hurst V, Ahluwalia A, Alam S, Avey MT, Baker M, et al. The arrive guidelines 2.0: updated guidelines for reporting animal research. *PLoS Biol.* (2020) 18:e3000410. doi: 10.1371/journal.pbio.3000410
- Ewels P, Magnusson M, Lundin S, Käller M. MultiQC: summarize analysis results for multiple tools and samples in a single report. *Bioinformatics.* (2016) 32:3047–8. doi: 10.1093/bioinformatics/btw354
- Bolger AM, Lohse M, Usadel B. Trimmomatic: a flexible trimmer for Illumina sequence data. *Bioinformatics.* (2014) 30:2114–20. doi: 10.1093/bioinformatics/btu170
- Kim D, Paggi JM, Park C, Bennett C, Salzberg SL. Graph-based genome alignment and genotyping with HISAT2 and HISAT-genotype. *Nat Biotechnol.* (2019) 37:907–15. doi: 10.1038/s41587-019-0201-4
- Li H, Handsaker B, Wysoker A, Fennell T, Ruan J, Homer N, et al. The sequence alignment/map format and SAMtools. *Bioinformatics.* (2009) 25:2078–9. doi: 10.1093/bioinformatics/btp352
- Kovaka S, Zimin AV, Perteau GM, Razaghi R, Salzberg SL, Perteau M. Transcriptome assembly from long-read RNA-seq alignments with StringTie2. *Genome Biol.* (2019) 20:278. doi: 10.1186/s13059-019-1910-1
- Perteau M, Kim D, Perteau GM, Leek JT, Salzberg SL. Transcript-level expression analysis of RNA-seq experiments with HISAT, StringTie and Ballgown. *Nat Protoc.* (2016) 11:1650–67. doi: 10.1038/nprot.2016.095
- McCarthy DJ, Chen Y, Smyth GK. Differential expression analysis of multifactor RNA-Seq experiments with respect to biological variation. *Nucleic Acids Res.* (2012) 40:4288–97. doi: 10.1093/nar/gks042
- Robinson MD, McCarthy DJ, Smyth GK. edgeR: a Bioconductor package for differential expression analysis of digital gene expression data. *Bioinformatics.* (2009) 26:139–40. doi: 10.1093/bioinformatics/btp616
- Zhang Y, Parmigiani G, Johnson WE. ComBat-seq: batch effect adjustment for RNA-seq count data. *NAR Genom Bioinform.* (2020) 2. doi: 10.1093/nargab/lqaa078
- Chen Y, Lun ATL, Smyth GK. From reads to genes to pathways: differential expression analysis of RNA-Seq experiments using Rsubread and the edgeR quasi-likelihood pipeline. *F1000Res.* (2016) 5:1438. doi: 10.12688/f1000research.8987.2
- Robinson MD, Oshlack A. A scaling normalization method for differential expression analysis of RNA-seq data. *Genome Biol.* (2010) 11:R25. doi: 10.1186/gb-2010-11-3-r25
- Rivellese F, Surace AEA, Goldmann K, Sciacca E, Çubuk C, Giorli G, et al. Rituximab versus tocilizumab in rheumatoid arthritis: synovial biopsy-based biomarker analysis of the phase 4 R4RA randomized trial. *Nat Med.* (2022) 28:1256–68. doi: 10.1038/s41591-022-01789-0
- Bu D, Luo H, Huo P, Wang Z, Zhang S, He Z, et al. KOBAS-i: intelligent prioritization and exploratory visualization of biological functions for gene enrichment analysis. *Nucleic Acids Res.* (2021) 49:W317–25. doi: 10.1093/nar/gkab447
- Fabregat A, Sidiropoulos K, Viteri G, Forner O, Marin-García P, Arnau V, et al. Reactome pathway analysis: a high-performance in-memory approach. *BMC Bioinformatics.* (2017) 18:142. doi: 10.1186/s12859-017-1559-2
- Kanehisa M, Goto S. KEGG: Kyoto encyclopedia of genes and genomes. *Nucleic Acids Res.* (2000) 28:27–30. doi: 10.1093/nar/28.1.27
- Benjamini Y, Hochberg Y. Controlling the false discovery rate: a practical and powerful approach to multiple testing. *J R Stat Soc B Stat Methodol.* (1995) 57:289–300. doi: 10.1111/j.2517-6161.1995.tb02031.x
- Khan A, Mathelier A. Intervene: a tool for intersection and visualization of multiple gene or genomic region sets. *BMC Bioinformatics.* (2017) 18:287. doi: 10.1186/s12859-017-1708-7
- Horn JL. A rationale and test for the number of factors in factor analysis. *Psychom Theory.* (1965) 30:179–85. doi: 10.1007/BF02289447
- Buja A, Eyuboglu N. Remarks on parallel analysis. *Multivariate Behav Res.* (1992) 27:509–40. doi: 10.1207/s15327906mbr2704_2
- Scott MA, Woolums AR, Swiderski CE, Finley A, Perkins AD, Nanduri B, et al. Hematological and gene co-expression network analyses of high-risk beef cattle defines immunological mechanisms and biological complexes involved in bovine respiratory disease and weight gain. *PLoS One.* (2022) 17:e0277033. doi: 10.1371/journal.pone.0277033
- Scott MA, Woolums AR, Swiderski CE, Perkins AD, Nanduri B, Smith DR, et al. Whole blood transcriptomic analysis of beef cattle at arrival identifies potential predictive molecules and mechanisms that indicate animals that naturally resist bovine respiratory disease. *PLoS One.* (2020) 15:e0227507. doi: 10.1371/journal.pone.0227507
- Punina NV, Makridakis NM, Remnev MA, Topunov AF. Whole-genome sequencing targets drug-resistant bacterial infections. *Hum Genomics.* (2015) 9:19. doi: 10.1186/s40246-015-0037-z
- Pietäinien M, François P, Hyryläinen HL, Tangomo M, Sass V, Sahl HG, et al. Transcriptome analysis of the responses of *Staphylococcus aureus* to antimicrobial peptides and characterization of the roles of vraDE and vraSR in antimicrobial resistance. *BMC Genomics.* (2009) 10:429. doi: 10.1186/1471-2164-10-429
- CCL C, Hurley DJ, Reber AJ. Neonatal Immune Development in the Calf and Its Impact on Vaccine Response. *Vet Clin North Am Food Anim Pract.* (2008) 24:87–104. doi: 10.1016/j.cvfa.2007.11.001
- Menge C, Neufeld B, Hirt W, Schmeer N, Bauerfeind R, Baljer G, et al. Compensation of preliminary blood phagocyte immaturity in the newborn calf. *Vet Immunol Immunopathol.* (1998) 62:309–21. doi: 10.1016/S0165-2427(98)00109-3
- Cortese VS. Neonatal Immunology. *Vet Clin North Am Food Anim Pract.* (2009) 25:221–7. doi: 10.1016/j.cvfa.2008.10.003
- Murray GM, More SJ, Sammin D, Casey MJ, McElroy MC, O'Neill RG, et al. Pathogens, patterns of pneumonia, and epidemiologic risk factors associated with respiratory disease in recently weaned cattle in Ireland. *J Vet Diagn Investig.* (2017) 29:20–34. doi: 10.1177/1040638716674757
- Callan RJ, Garry FB. Biosecurity and bovine respiratory disease. *Vet Clin North Am Food Anim Pract.* (2002) 18:57–77. doi: 10.1016/S0749-0720(02)00004-X
- Carroll JA, Forsberg NE. Influence of stress and nutrition on cattle immunity. *Vet Clin North Am Food Anim Pract.* (2007) 23:105–49. doi: 10.1016/j.cvfa.2007.01.003
- Ci X, Song Y, Zeng F, Zhang X, Li H, Wang X, et al. Ceftiofur impairs pro-inflammatory cytokine secretion through the inhibition of the activation of NF-κB and MAPK. *Biochem Biophys Res Commun.* (2008) 372:73–7. doi: 10.1016/j.bbrc.2008.04.170
- Ci X, Chu X, Chen C, Li X, Yan S, Wang X, et al. Oxytetracycline attenuates allergic airway inflammation in mice via inhibition of the NF-κB pathway. *J Clin Immunol.* (2011) 31:216–27. doi: 10.1007/s10875-010-9481-7
- Ichiyama T, Nishikawa M, Yoshitomi T, Hasegawa S, Matsubara T, Hayashi T, et al. Clarithromycin inhibits NF-κB activation in human peripheral blood mononuclear cells and pulmonary epithelial cells. *Antimicrob Agents Chemother.* (2001) 45:44–7. doi: 10.1128/AAC.45.1.44-47.2001
- Klaudia C, Alina W. The influence of enrofloxacin, florfenicol, ceftiofur and *E. coli* LPS interaction on T and B cells subset in chicks. *Vet Res Commun.* (2015) 39:53–60. doi: 10.1007/s11259-015-9632-7

50. Abraham RT, Wiederrecht GJ. Immunopharmacology of rapamycin. *Annu Rev Immunol.* (1996) 14:483–510. doi: 10.1146/annurev.immunol.14.1.483
51. Platania CBM, Ronchetti S, Riccardi C, Migliorati G, Marchetti MC, Di Paola L, et al. Effects of protein-protein interface disruptors at the ligand of the glucocorticoid-induced tumor necrosis factor receptor-related gene (GITR). *Biochem Pharmacol.* (2020) 178:114110. doi: 10.1016/j.bcp.2020.114110
52. Tang X, Tian J, Ma J, Wang J, Qi C, Rui K, et al. GITRL modulates the activities of p38 MAPK and STAT3 to promote Th17 cell differentiation in autoimmune arthritis. *Oncotarget.* (2015) 7:8590–600. doi: 10.18632/oncotarget.6535
53. Lindenberg M, Almeida L, Dhillon-Labrooy A, Siegel E, Henriques-Normark B, Sparwasser T. Clarithromycin impairs tissue-resident memory and Th17 responses to macrolide-resistant *Streptococcus pneumoniae* infections. *J Mol Med.* (2021) 99:817–29. doi: 10.1007/s00109-021-02039-5
54. Zanni MP, Von Greyerz S, Schnyder B, Brander KA, Frutig K, Hari Y, et al. HLA-restricted, processing- and metabolism-independent pathway of drug recognition by human T lymphocytes. *J Clin Invest.* (1998) 102:1591–8. doi: 10.1172/JCI3544
55. Padovan E, Bauer T, Tongio MM, Kalbacher H, Weltzien HU. Penicilloyl peptides are recognized as T cell antigenic determinants in penicillin allergy. *Eur J Immunol.* (1997) 27:1303–7. doi: 10.1002/eji.1830270602
56. Loureiro J, Ploegh HL. Antigen presentation and the ubiquitin-proteasome system in host-pathogen interactions. *Adv Immunol.* (2006) 92:225–305. doi: 10.1016/S0065-2776(06)92006-9
57. Zenobia C, Hajishengallis G. Basic biology and role of interleukin-17 in immunity and inflammation. *Periodontol.* (2000) 69:142–59. doi: 10.1111/prd.12083
58. Żyżyńska-Granica B, Trzaskowski B, Dutkiewicz M, Zegrocka-Stendel O, Machcińska M, Bocian K, et al. The anti-inflammatory potential of cefazolin as common gamma chain cytokine inhibitor. *Sci Rep.* (2020) 10:2886. doi: 10.1038/s41598-020-59798-3
59. Fischer CD, Beatty JK, Duquette SC, Morck DW, Lucas MJ, Buret AG. Direct and indirect anti-inflammatory effects of tulathromycin in bovine macrophages: inhibition of CXCL-8 secretion, induction of apoptosis, and promotion of efferocytosis. *Antimicrob Agents Chemother.* (2013) 57:1385–93. doi: 10.1128/AAC.01598-12
60. Fischer CD, Beatty JK, Zvaigzne CG, Morck DW, Lucas MJ, Buret AG. Anti-inflammatory benefits of antibiotic-induced neutrophil apoptosis: Tulathromycin induces caspase-3-dependent neutrophil programmed cell death and inhibits NF- κ B signaling and CXCL8 transcription. *Antimicrob Agents Chemother.* (2011) 55:338–48. doi: 10.1128/AAC.01052-10
61. Fischer CD, Duquette SC, Renaux BS, Feener TD, Morck DW, Hollenberg MD, et al. Tulathromycin exerts proresolving effects in bovine neutrophils by inhibiting phospholipases and altering leukotriene B₄, prostaglandin E₂, and lipoxin A₄ production. *Antimicrob Agents Chemother.* (2014) 58:4298–307. doi: 10.1128/AAC.02813-14
62. De Lamache DD, Moges R, Siddiq A, Allain T, Feener TD, Muench GP, et al. Immuno-modulating properties of Tulathromycin in porcine monocyte-derived macrophages infected with porcine reproductive and respiratory syndrome virus. *PLoS One.* (2019) 14:e0221560. doi: 10.1371/journal.pone.0221560
63. Abdel-Motal S, Shams G, Edress N, Anwer A, Mohamed G. Immunomodulatory effects of Tulathromycin in rabbits. *Zagazig Vet J.* (2017) 45:1–10. doi: 10.21608/zvjz.2017.7681
64. Rutenberg D, Venner M, Giguère S. Efficacy of Tulathromycin for the treatment of foals with mild to moderate bronchopneumonia. *J Vet Intern Med.* (2017) 31:901–6. doi: 10.1111/jvim.14717
65. Menge M, Rose M, Bohland C, Zschiesche E, Kilp S, Metz W, et al. Pharmacokinetics of tildipirosin in bovine plasma, lung tissue, and bronchial fluid (from live, nonanesthetized cattle). *J Vet Pharmacol Ther.* (2012) 35:550–9. doi: 10.1111/j.1365-2885.2011.01349.x
66. Datta C, Das D, Mondal P, Chakraborty B, Sengupta M, Bhattacharjee CR. Novel water soluble neutral vanadium(IV)-antibiotic complex: antioxidant, immunomodulatory and molecular docking studies. *Eur J Med Chem.* (2015) 97:214–24. doi: 10.1016/j.ejmech.2015.05.005
67. Yao M, Gao W, Tao H, Yang J, Huang T. The regulation effects of danofloxacin on pig immune stress induced by LPS. *Res Vet Sci.* (2017) 110:65–71. doi: 10.1016/j.rvsc.2016.11.005
68. Yu C-H, Liu Z-Y, Sun L-S, Li Y-J, Zhang D-S, Pan R-T, et al. Effect of Danofloxacin on reactive oxygen species production, lipid peroxidation and antioxidant enzyme activities in kidney tubular epithelial cell line, LLC-PK1. *Basic Clin Pharmacol Toxicol.* (2013) 113:377–84. doi: 10.1111/bcpt.12110
69. Li P, Ye J, Zeng S, Yang C. Florfenicol alleviated lipopolysaccharide (LPS)-induced inflammatory responses in *Ctenopharyngodon idella* through inhibiting toll / NF- κ B signaling pathways. *Fish Shellfish Immunol.* (2019) 94:479–84. doi: 10.1016/j.fsi.2019.08.073
70. Zhang X, Xiong H, Li H, Yu L, Deng X. Effects of florfenicol on LPS-induced nitric oxide and prostaglandin E₂ production in RAW 264.7 macrophages: effects of florfenicol on nitric oxide and prostaglandin E₂. *Fundam Clin Pharmacol.* (2011) 25:591–8. doi: 10.1111/j.1472-8206.2010.00886.x
71. Shuang G, Yu S, Weixiao G, Dacheng W, Zhichao Z, Jing L, et al. Immunosuppressive activity of Florfenicol on the immune responses in mice. *Immunol Investig.* (2011) 40:356–66. doi: 10.3109/08820139.2010.551434
72. Zhang X, Song K, Xiong H, Li H, Chu X, Deng X. Protective effect of florfenicol on acute lung injury induced by lipopolysaccharide in mice. *Int Immunopharmacol.* (2009) 9:1525–9. doi: 10.1016/j.intimp.2009.09.007
73. Venditto VJ, Haydar D, Abdel-Latif A, Gensel JC, Anstead MI, Pitts MG, et al. Immunomodulatory effects of azithromycin revisited: potential applications to COVID-19. *Front Immunol.* (2021) 12:574425. doi: 10.3389/fimmu.2021.574425
74. Iula L, Keitelman IA, Sabbione F, Fuentes F, Guzman M, Galletti JG, et al. Autophagy mediates interleukin-1 β secretion in human neutrophils. *Front Immunol.* (2018) 9:269. doi: 10.3389/fimmu.2018.00269
75. Sha L-L, Wang H, Wang C, Peng H-Y, Chen M, Zhao M-H. Autophagy is induced by anti-neutrophil cytoplasmic abs and promotes neutrophil extracellular traps formation. *Innate Immun.* (2016) 22:658–65. doi: 10.1177/1753425916668981